Hydrogeology Journal (2015) 23: 287–303
DOI 10.1007/s10040-014-1191-4

# Baseflow recession analysis in the inland Pacific Northwest of the United States

**R. Sánchez-Murillo · E. S. Brooks · W. J. Elliot · E. Gazel · J. Boll**

**Abstract** The storage-discharge relationships of 26 watersheds in the inland Pacific Northwest of the United States were analyzed. Four fitting methods were used to obtain the baseflow coefficients: lower envelope, organic correlation, and ordinary and inverse least squares. Several climatic and terrain attributes were evaluated as predictors of baseflow coefficients. Watersheds dominated by basalt and flatter landscapes exhibited the smallest recession time scales ($K$) (12.5–20.0 days). Greater $K$ values (33.3–66.7 days) were obtained over catchments dominated by metamorphic and sedimentary rocks. Mean basin slope and the aridity index were found to be the best estimators of baseflow coefficients. Baseflow in flat basalt landscapes, located in dry warm climates, decrease rapidly during summer months and are most sensitive to future droughts and warming climates. Groundwater systems feeding streams during the driest months can drop to less than 1 mm of effective storage in these sensitive systems. In contrast, the minimum annual storage in mountainous systems can have greater than 10 mm effective storage. By understanding the main factors controlling baseflow recession characteristics, environmental agencies could prioritize efforts in areas where future droughts and land use changes may affect ecological assemblages and socio-economic activities.

**Keywords** USA · Groundwater/surface-water relations · Geology · Climate · Watershed management

Received: 4 April 2014 / Accepted: 31 August 2014
Published online: 11 October 2014



**Electronic supplementary material** The online version of this article (doi:10.1007/s10040-014-1191-4) contains supplementary material, which is available to authorized users.

R. Sánchez-Murillo · J. Boll
Waters of the West – Water Resources Program, University of Idaho, Moscow, ID 83844-3006, USA

R. Sánchez-Murillo (✉)
Chemistry Department, Universidad Nacional, Heredia, P.O. Box 86-3000, Costa Rica
e-mail: sanc7767@vandals.uidaho.edu
Tel.: +506.2277-3351

E. S. Brooks · J. Boll
Department of Biological and Agricultural Engineering, University of Idaho, Moscow, ID 83844-2060, USA

W. J. Elliot
USDA Forest Service Rocky Mountain Research Station, Moscow, ID 83843, USA

E. Gazel
Department of Geosciences, Virginia Tech, Blacksburg, VA 24061, USA

## Introduction

Climate change is expected to increase evaporation and precipitation across the globe resulting in an intensification or acceleration of the water cycle in the coming decades (Del Genio et al. 1991; Nijssen et al. 2001; Huntington 2006; Durack et al. 2012), which may significantly alter the magnitude and timing of streamflow regimes (Tang and Lettenmaier 2012; Döll and Zhang 2010; Döll and Müller-Schmied 2012; Arnell and Gosling 2013). Consequently, international efforts (e.g. International Flood Initiative; UNESCO 2005) and government attention has been geared to prevent and mitigate the effects of extreme flood events (Plate 2002), especially in developing countries. A broad spectrum of human activities (e.g. food production, drinking water, recreation) and ecological assemblages (e.g. habitat volume for aquatic biota, biochemistry and thermal regimes) rely on sustained baseflow conditions. Despite its importance, however, current understanding of future impacts on long-term groundwater storage and baseflow regimes is limited (Dams et al. 2012; Brutsaert 2012).

Baseflow is described as the cumulative outflow from all upstream riparian aquifers during rainless periods, in the absence of snowmelt or any other hydrologic inputs such as return irrigation return flows (Brutsaert 2005). Changes in groundwater storage and baseflow discharge constitute a critical component of any ecosystem. For example, baseflow plays an important role in regulating stream chemistry, water temperature and dissolved oxygen during critical summer months, and provides continuous habitat volume to endangered aquatic species in temperate

regions (Sánchez-Murillo et al. 2013). Furthermore, information on baseflow characteristics and groundwater storage is important for decision making related to effective allocation of resources, water-quality-standard assessments and regulations, and prioritization of water conservation efforts in areas of accelerated potential future droughts or population growth.

The Pacific Northwest of the United States (PNW) has been recognized as a particularly sensitive region to climate variability (Miles et al. 2000; Elsner et al. 2010). Since the 1940s, a decreasing trend in snow water equivalent has been observed while water consumption has increased (Mote 2003; Stewart et al. 2005; McCabe and Clark 2005; Van Kirk and Naman 2008). Overall, a consensus exists that snow-dominated watersheds within the PNW will potentially experience spring runoff episodes up to 4 weeks earlier. Future climate scenarios for the PNW (Mote and Salathé 2010) project a warming of 0.1–0.6 °C per decade. Furthermore, Mayer (2012) found that baseflow is one of the major factors controlling summer thermal regimes across the region with a mean sensitivity of 0.47 °C (stream)/°C (air). Stream water temperature is a function of heat load and discharge volume (i.e. water temperature $\propto$ heat load/discharge); consequently, an increase of air temperature and decline in baseflow discharge may cause the disruption of stream thermal regimes especially throughout the summer (Poole and Berman 2001), indicating a need to improve our understanding of how seasonal variability in baseflow impacts stream environments.

Over the last half century, the PNW has been experiencing declines in summer baseflow. Clark (2010) found a decrease of 25 % in daily minimum streamflow across Idaho, western Wyoming, and northern Nevada. Luce and Holden (2009) examined 43 stream stations throughout the PNW and found a significant decline in the 25th percentile of annual flow in 72 % of the stations. Half the stream stations showed a 29 % decline in the 25th percentile of flow between 1948 and 2006 with records from one station indicating a 47 % drop. Leppi et al. (2012) examined 50-year records from 153 stream stations in the Central Rocky Mountain Region and found declining trends in the mean monthly flow in August in 89 % of the stations. Fu et al. (2010) noted similar differences in mean annual flow at 35 stations in Washington State. In a recent study of 420 catchments across the contiguous United States, Berghuijs et al. (2014) indicated that annual fraction of precipitation falling as snow has a significant influence on the mean annual streamflow, independent of precipitation amount; therefore, a precipitation shift from snow towards a rain-dominated regime significantly decreases the mean streamflow. Understanding long-term patterns of baseflow recession emerges as a fundamental mission. It is essential that new methods are developed to support future decisions responding to how accelerated population growth and climate variability may impact water distribution systems in the PNW and elsewhere (Milly et al. 2005; Huntington 2006; Bates et al. 2008; Zhou et al. 2011).

This study analyzed the storage-discharge relationships across 26 watersheds in the inland PNW with a variety of basin areas, geologic formations, land uses, and temperature and precipitation gradients. A modified methodology for baseflow analysis applicable for steep and flat landscapes is presented. This study presents the first baseflow recession analysis for the inland PNW. The specific objectives were: (1) to evaluate the main terrain characteristics controlling the natural release of water as baseflow; (2) to estimate the role that climate plays in the baseflow recession process; and (3) to determine the regional variability of the recession time scale ($K$) and minimum annual storage across the inland PNW.

## Baseflow recession analyses methods

Generally, baseflow is examined using low frequency analysis such as $Q_{7,10}$ (i.e. 7-day, 10-year return period discharge) (Vogel and Kroll 1992; Brandes et al. 2005), baseflow indices (Wolock 2003; Bloomfield et al. 2009), and recession analysis methods (Tallaksen 1995). Detailed reviews of recession analysis have been reported elsewhere (Hall 1968; Wittenberg 1999; Smakhtin 2001; Kirchner 2009; Price 2011). To overcome the uncertainties involved in defining the time at which the recession begins, Brutsaert and Nieber (1977) proposed a method to parameterize a storage-discharge relationship based on the Boussinesq equation (i.e. flow from an unconfined horizontal aquifer). The solution to the problem of outflow from an unconfined rectangular aquifer on a horizontal impermeable layer into a fully penetrating stream channel was proposed by Boussinesq (1877). The solution assumes that the water table is a free surface and neglects the effects of capillarity above the water table. It also relies on Dupuit assumptions, specifically that: (1) flow is parallel to the bed slope, (2) the velocity is uniform perpendicular to the bed, and (3) the hydraulic gradient equals the slope of the free surface. In this application, the slope of the impermeable bed is neglected and assumed to be horizontal.

Brutsaert and Nieber (1977) method consists of plotting the decline in discharge ($-dQ/dt$) [L $T^{-2}$] versus average discharge ($Q$) [L $T^{-1}$] (Eq. 1; Fig. 1). The main advantage of representing the recession curve in the form shown in Eq. (1) is the elimination of time as a dependent variable; thus, it is unnecessary to select the precise beginning of the recession.

$$-\frac{dQ}{dt} = f(Q) \tag{1}$$

where $f$ is a characteristic function for a given watershed and $Q$ [L/T] is streamflow. When using actual discharge data, Eq. (1) can be expressed as follows:

$$\frac{Q_i - Q_{i-1}}{\Delta t} = f\left(\frac{Q_i + Q_{i+1}}{2}\right) \tag{2}$$


DOI 10.1007/s10040-014-1191-4

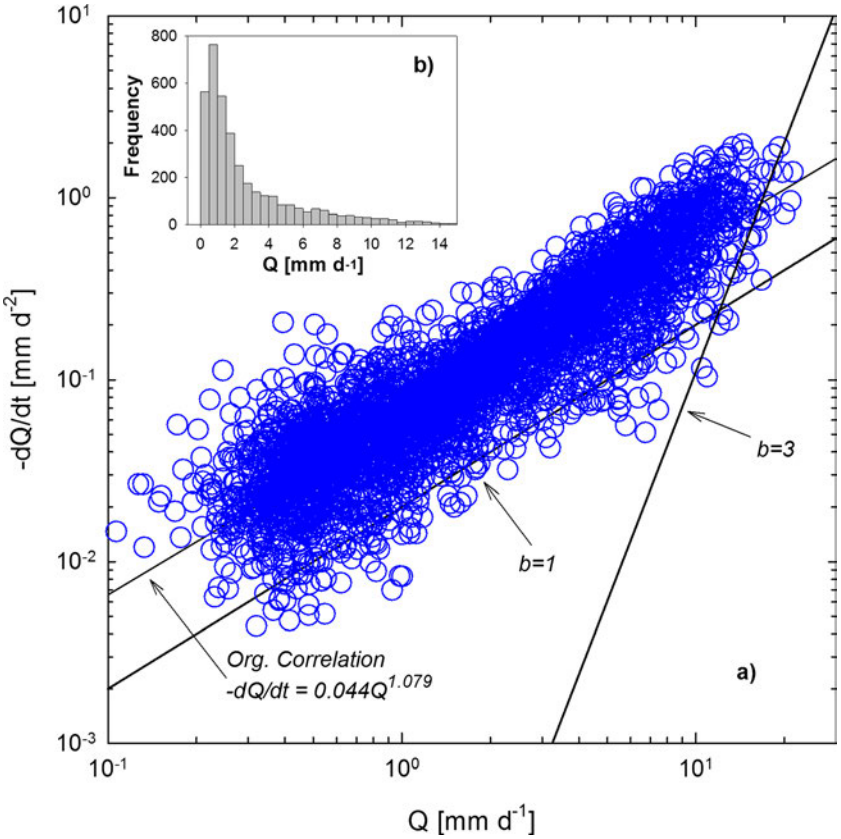


**Fig. 1** **a** Natural spectrum of data points showing decline in discharge, $-dQ/dt$ [mm $d^{-2}$], versus the average discharge, $Q$ [mm $d^{-1}$], during the period 1939–2011 on Lochsa River, Lowell, Idaho. The drainage area is 3,060 $km^2$. The lower envelopes are represented by the lines with slopes $b=1$ and $b=3$. The organic correlation fitting method exhibits a slope of 1.079. **b** Shows the distribution of average discharge $Q$ [mm $d^{-1}$]

where the subscript $i$ represents a counter in the discharge time series. Change in underground water storage in a particular watershed over a period of time is described by the conservation of mass equation:

$$\frac{dS}{dt} = P - \mathrm{ET} - Q - L \tag{3}$$

where $S$ [L] is the volume of water stored in the watershed, $P$ [$LT^{-1}$] is precipitation, ET [$LT^{-1}$] is evapotranspiration, $Q$ [$LT^{-1}$] is discharge, and $L$ [$LT^{-1}$] is lateral flow. In the absence of aquifer recharge, when $P$, ET, and $L$ are negligible, baseflow dominates stream discharge and Eq. (3) can be written as:

$$\frac{dS}{dt} = -Q \tag{4}$$

Linear reservoir theory assumes that outflow $Q$ from the bedrock or riparian aquifer is linearly dependent on the storage $S$ (Tallaksen 1995):

$$Q = \mathrm{a}S \tag{5}$$

where a is a constant [$T^{-1}$]. Substituting Eq. (5) into Eq. (4), the mass balance equation yields a power law relationship between $-dQ/dt$ and discharge $Q$:

$$-\frac{dQ}{dt} = \mathrm{a}Q^b \tag{6}$$

where $b$ is an exponent; $b=1$ yields the linear reservoir special case. One of the advantages of representing the recession process in a power form such as Eq. (6) is that three well-known analytical solutions (Table 1) to the Boussinesq equation for an unconfined horizontal aquifer can also be expressed in a power form where coefficient $a$ is a function of the hydraulic properties of the system.

Equation (6) can be also log-transformed to:

$$\log(-dQ/dt) = \log(a) + b\log(Q) \tag{7}$$

In the method of Brutsaert and Nieber (1977), when plotting the decline in discharge ($-dQ/dt$) [$LT^{-2}$] versus average discharge ($Q$) [$L\,T^{-1}$] on a log-log scale a natural cloud of data points is obtained, where the lower envelope represents the lowest $dQ/dt$ for a given $Q$ (Fig. 1). The lower envelope can be analyzed using three fixed slopes $b$ equal to 1, 1.5, and 3 (Brutsaert and Lopez 1998). A slope of 1 represents a linearized outflow from a rectangular aquifer into a fully penetrated channel. A slope of 1.5 describes a situation in which the shape of the water table remains curvilinear for a long time. Finally, a slope of 3


DOI 10.1007/s10040-014-1191-4

**Table 1** Solutions to Boussinesq equation for an unconfined horizontal aquifer

| Linearity | Time domain | Slope $b$ | Outflow time $a$ ($L^{1-b}T^{-1}$) | Source |
|---|---|---|---|---|
| Non-linear | Short | 3 | $\frac{1.1334}{k\varphi D^3 L^2}$ | Polubarinova-Kochina (1962) |
| Non-linear | Long | 1.5 | $\frac{4.804k^{1/2}L}{\varphi A^{3/2}}$ | Boussinesq (1904) |
| Linearized | Long | 1 | $\frac{\pi p k D L^2}{\varphi A^2}$ | Boussinesq (1903) |

$k$ hydraulic conductivity, $\varphi$ drainable porosity, $D$ aquifer depth, $L$ upstream length, $A$ drainage area, $p$ is a constant (0.3465)

describes a high flow scenario based on the assumption that the aquifer boundary at the divide stays infinitely distant from the channel (Brutsaert and Lopez 1998; Brutsaert 2005).

The selection of the exact lower envelope position has also been a matter of discussion (Ajami et al. 2011; Stoelzle et al. 2012), because there is some degree of subjectivity or uncertainty related with this procedure. Kirchner (2009) suggested estimating the central tendency of $-dQ/dt$ instead of the lower envelope as a better average descriptor of a watershed's natural behavior. Several fitting techniques have been used to estimate the baseflow coefficients (i.e. $a$ and $b$) from linear regression models (Brutsaert and Lopez 1998) to binning means (Parlange et al. 2001; Kirchner 2009; Palmroth et al. 2010), and mean relative errors (Peña-Arancibia et al. 2010; van Dijk 2010). Rupp and Selker (2006) reported that the lower envelope may be affected by precision and noise in the streamflow data causing scattering and discretization at low flows. These two factors, illustrated by the horizontal artifacts when plotting $-dQ/dt$ versus average discharge $Q$ (Fig. 2), may lead to misinterpretation of the recession phenomena.

Despite the variety of approaches used to determine the baseflow coefficients, the Brutsaert and Nieber (1977) method has been successfully used to determine basin-scale effective groundwater parameters (i.e. aquifer thickness, hydraulic conductivity, drainage porosity; Zecharias and Brutsaert 1988; Troch et al. 1993; Brutsaert and Lopez 1998; Szilagyi et al. 1998; Mendoza et al. 2003); mountain block recharge (Ajami et al. 2011), human influences on baseflow (Wittenberg 2003; Wang and Cai 2009; 2010a, b), and long-term minimum annual storage trends (Brutsaert 2008, 2012; Brutsaert and Sugita 2008). The latter application provides meaningful information to evaluate water management under changing climate conditions and may be a potential tool to estimate water availability in ungauged basins.

The minimum annual storage in a particular basin can be evaluated as:

$$S = Ky \tag{8}$$

where $y=Q/A$ is the rate of flow ($Q$) per unit of drainage area ($A$) [$LT^{-1}$] and $K$ (i.e. $a^{-1}$, see Eq. 5) is the characteristic recession time scale [T]. Basically, $K$ represents mainly the groundwater drainage characteristic of a particular watershed. Since the rate of flow per unit area continually changes during the year, it's necessary to evaluate which value of the baseflows best reflects the annual value of the basin minimum storage. Brutsaert (2012) reported the annual lowest 7-day daily mean flow ($y_{L7}$) as a robust measure to evaluate the minimum annual basin storage. Additionally, several studies (Brutsaert 2008, 2010, 2012; Brutsaert and Sugita 2008) have found on average a $K$ of 45 days with an uncertainty of 15 days for large basins (i.e. >100 $km^2$). Brutsaert and Lopez (1998) found a mean $K$ of 31.6 days for 22 subbasins in the southern Great Plains of the United States with extremes of 12.5 and 66.5 days.

## Materials and methods

### Data selection and watersheds characteristics

Long-term daily discharge and precipitation records were obtained for 26 watersheds throughout eastern Washington and central and northern Idaho (Fig. 3; Tables 2 and 3) from the United States Geological Survey National Water Information System (USGS 2011) and the National Oceanic and Atmospheric Administration (NOAA 2011), respectively. Total discharge and precipitation records ranged from 7 to 75 years with a mean length of 33 years. In selecting the watersheds, hydrological alterations such as dams, reservoirs, irrigation, and return flows were avoided. Therefore, most of the watersheds represent near-natural conditions corresponding to inter-mountainous forested or semi-arid areas. Daily streamflow records were normalized to unit area discharge [$L\ T^{-1}$].

Several geomorphic and climatic attributes were determined for each watershed (Tables 2 and 3) based on digital elevation models (30×30 m, Seamless, USGS) and the Parameter-Elevation Regressions on Independent Slopes Model (PRISM, Climate Group, USA) using ArcGIS version 9.3.1. (ESRI, USA). The study watersheds cover a wide range of climate gradients and terrain characteristics. A detailed summary of main underlying geology in each watershed is presented in Table 4 and Fig. 4.

### Recession extraction and analysis

To ensure comparability of the recession analysis, several procedures were applied according to the Brutsaert and Nieber (1977) method. Data points within a recession period were extracted in accordance with the following steps: (1) positive or zero $dQ/dt$ values were eliminated; (2) $-dQ/dt$ values were only considered after 3 days of any precipitation event, to avoid the influence of surface flows; (3) days with


DOI 10.1007/s10040-014-1191-4

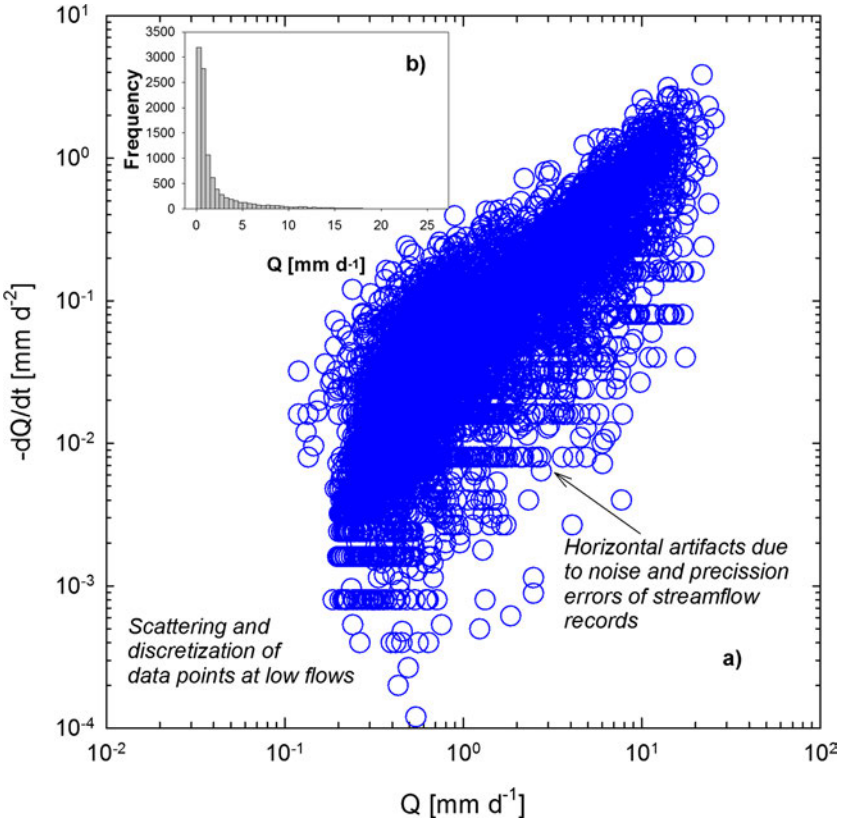


**Fig. 2** **a** Example of horizontal artifacts due to noise and precision errors of streamflow records at lower flow rates when plotting $-dQ/dt$ [mm $d^{-2}$] versus the average $Q$ [mm $d^{-1}$] during the period 1939–2011 on Lochsa River, Lowell, Idaho. The drainage area is 3,060 $km^2$. **b** Shows the distribution of average discharge $Q$ [mm $d^{-1}$]

recorded precipitation were excluded; (4) due to precision errors at low flows, a trial and error threshold was applied ($1-Q_{i+n}/Q_i>0.1$) to avoid horizontal artifacts (i.e. effect of precision of stage height and streamflow values), where $Q_i$ is the initial discharge and $Q_{i+n}$ is the discharge corresponding to the selected time step ($dt$).

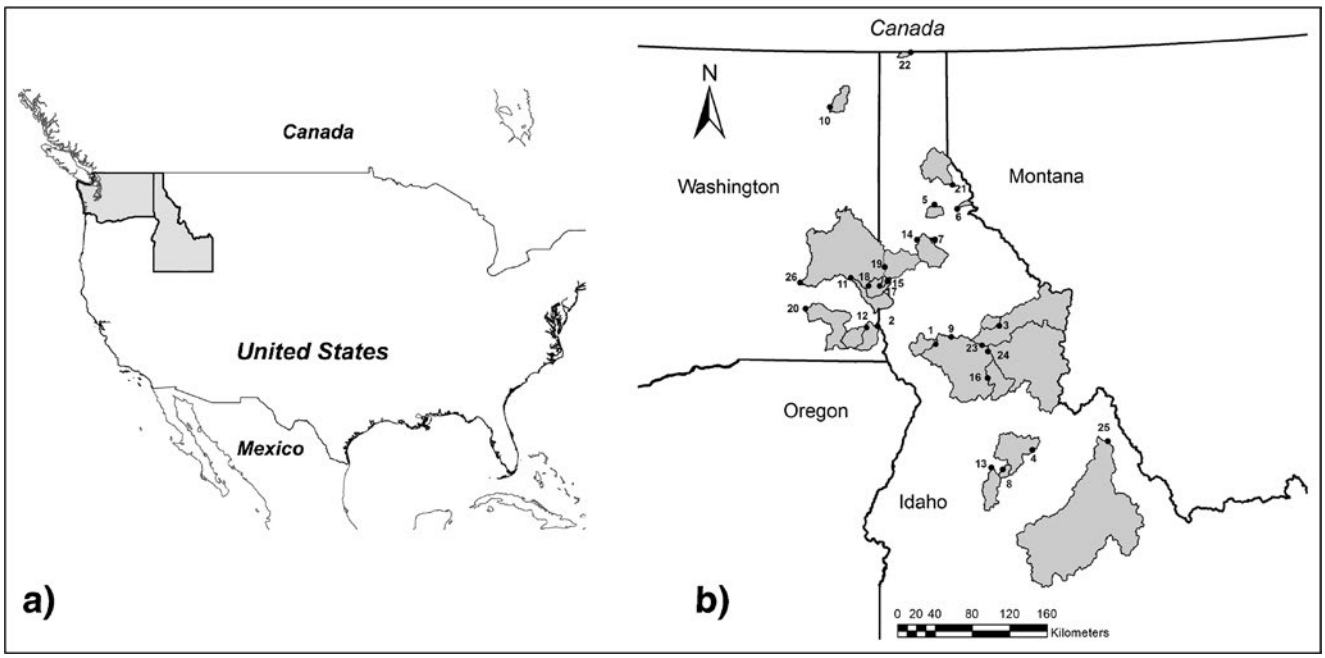


**Fig. 3** **a** Location of Washington (*WA*) and Idaho (*ID*) states within the Pacific Northwest of the United States. **b** Study area including watershed outlets (numbered *black dots*; see Table 2) boundaries (*black lines*) across eastern Washington and northern/central Idaho

 DOI 10.1007/s10040-014-1191-4

Hydrogeology Journal (2015) 23: 287–303

**Table 2** Summary of geomorphic and climatic watershed (1–13) characteristics

| ID | Watershed | USGS ID | Period | Q [mm/year] | ET [mm/year] | P [mm/year] | AI | Mean T. [°C] | Mean slope [%] | Mean elevation [m] | Area [km$^2$] | Total stream length [km] | Drainage density | Total relief [m] |
|---|---|---|---|---|---|---|---|---|---|---|---|---|---|---|
| 1 | Lawyer Creek | 13338800 | 1967–1974 | 109 | 473 | 582 | 1.23 | 6.78 | 9.24 | 1,192 | 368 | 460 | 1.25 | 927 |
| 2 | Asotin Creek | 13334500 | 2001–2011 | 186 | 419 | 605 | 1.44 | 8.08 | 37.54 | 1,187 | 269 | 760 | 2.83 | 1,478 |
| 3 | Fish Creek | 13336900 | 1957–1967 | 109 | 1,202 | 1,311 | 1.09 | 5.77 | 36.11 | 1,360 | 228 | 310 | 1.36 | 1,409 |
| 4 | Big Creek | 13310000 | 1948–1958 | 406 | 480 | 886 | 1.85 | 1.84 | 45.70 | 2,130 | 1,168 | 1,358 | 1.16 | 1,647 |
| 5 | Pine Creek | 12413445 | 1998–2010 | 703 | 522 | 1,225 | 2.35 | 5.46 | 46.53 | 1,221 | 190 | 231 | 1.22 | 1,240 |
| 6 | Canyon Creek | 12413125 | 1998–2010 | 754 | 559 | 1,313 | 2.35 | 3.81 | 46.29 | 1,515 | 60 | 64 | 1.06 | 1,220 |
| 7 | Mica Creek | NA | 1991–2004 | 502 | 786 | 1,288 | 1.64 | 5.67 | 29.92 | 1,241 | 12.25 | 12 | 1.00 | 476 |
| 8 | Salmon River, Stibnite | 13311000 | 1982–1997 | 472 | 470 | 942 | 2.00 | 1.30 | 41.66 | 2,320 | 50 | 105 | 2.11 | 1,037 |
| 9 | Clearwater River, Kamiah | 13339000 | 1948–1965 | 591 | 473 | 1,064 | 2.25 | 4.79 | 37.22 | 1,511 | 12,357 | 15,733 | 1.27 | 2,501 |
| 10 | Little Pend Oreille River | 12408300 | 1958–1976 | 155 | 687 | 842 | 1.23 | 5.53 | 19.77 | 1,056 | 342 | 623 | 1.82 | 1,109 |
| 11 | Union Flat Creek | 13350500 | 1953–1971 | 155 | 461 | 616 | 1.34 | 8.51 | 11.19 | 820 | 489 | 801 | 1.64 | 556 |
| 12 | Asotin Creek | 13335050 | 1991–2010 | 103 | 420 | 523 | 1.25 | 8.55 | 28.02 | 1,025 | 836 | 1,382 | 1.65 | 1,659 |
| 13 | Johnson Creek | 13313000 | 1988–2010 | 522 | 593 | 1,115 | 1.88 | 1.79 | 28.90 | 2,175 | 564 | 568 | 1.01 | 1,362 |

**Table 3** Summary of geomorphic and climatic watershed (14-26) characteristics

| ID | Watershed | USGS ID | Period | Q [mm/yr] | ET [mm/yr] | P [mm/yr] | AI | Mean T. [°C] | Mean Slope [%] | Mean Elevation [m] | Area [km$^2$] | Total stream length [km] | Drainage density | Total Relief [m] |
|---|---|---|---|---|---|---|---|---|---|---|---|---|---|---|
| 14 | Saint Maries River | 12414900 | 1965-1988 | 443 | 682 | 1125 | 1.65 | 6.12 | 26.14 | 1095 | 699 | 1445 | 2.07 | 1155 |
| 15 | Crumarine Creek | NA | 1956-1983 | 230 | 801 | 1031 | 1.29 | 7.27 | 28.44 | 1121 | 6.35 | 8 | 1.29 | 659 |
| 16 | SF Clearwater River | 13337500 | 1950-1974, 2002-2010 | 342 | 637 | 979 | 1.54 | 4.27 | 25.10 | 1553 | 676 | 989 | 1.46 | 1098 |
| 17 | Paradise Creek | 13346800 | 1978-2011 | 146 | 601 | 747 | 1.24 | 8.02 | 12.67 | 866 | 45 | 60 | 1.33 | 552 |
| 18 | SF Palouse River | 13348000 | 19341942, 1960-1981, 2001-2005 | 97 | 573 | 670 | 1.17 | 8.22 | 12.02 | 832 | 342 | 586 | 1.71 | 807 |
| 19 | Palouse River, Potlatch | 13345000 | 1966-2010 | 283 | 567 | 850 | 1.50 | 6.96 | 22.32 | 965 | 821 | 1322 | 1.61 | 872 |
| 20 | Tucannon River | 13344500 | 1958-2010 | 146 | 518 | 664 | 1.28 | 8.90 | 26.96 | 896 | 1116 | 1821 | 1.63 | 1715 |
| 21 | NF Couer D'Alene River | 12411000 | 1950-2009 | 720 | 505 | 1225 | 2.43 | 5.23 | 42.20 | 1203 | 858 | 1259 | 1.47 | 1138 |
| 22 | Boundary Creek | 12321500 | 1947-2008 | 416 | 551 | 967 | 1.75 | 4.24 | 36.36 | 1361 | 428 | 237 | 0.09 | 1562 |
| 23 | Lochsa River | 13337000 | 1939-2011 | 817 | 481 | 1298 | 2.70 | 4.28 | 39.53 | 1583 | 3060 | 3279 | 1.07 | 2240 |
| 24 | Selway River | 13336500 | 1940-2011 | 666 | 449 | 1115 | 2.48 | 3.92 | 45.33 | 1680 | 4950 | 6470 | 1.31 | 2365 |
| 25 | Salmon River, Salmon | 13302500 | 1937-2010 | 175 | 411 | 586 | 1.43 | 2.80 | 34.44 | 2255 | 9740 | 14117 | 1.45 | 2660 |
| 26 | Palouse River, Hooper | 13351000 | 1900-1916 1951-2010 | 85 | 461 | 546 | 1.18 | 8.51 | 12.19 | 727 | 6472 | 9195 | 1.42 | 1301 |

DOI 10.1007/s10040-014-1191-4

**Table 4** Summary of main geologic features in the study watersheds

| Watershed | Percent of main geologic features | | | | | | | | | |
|---|---|---|---|---|---|---|---|---|---|---|
| | Alluvial | Granitic | Basalt | Eolian | Mafic | Metamorphic | Sedimentary | Glacial drift | Volcanic | Unconsolidated material |
| 1. Lawyer Creek | 0.0 | 12.3 | 77.1 | 0.0 | 0.0 | 10.6 | 0.0 | 0.0 | 0.0 | 0.0 |
| 2. Asotin Creek | 0.0 | 0.0 | 0.0 | 4.8 | 95.2 | 0.0 | 0.0 | 0.0 | 0.0 | 0.0 |
| 3. Fish Creek | 0.0 | 100.0 | 0.0 | 0.0 | 0.0 | 0.0 | 0.0 | 0.0 | 0.0 | 0.0 |
| 4. Big Creek | 0.6 | 38.0 | 0.0 | 0.0 | 0.0 | 27.1 | 0.0 | 0.0 | 34.3 | 0.0 |
| 5. Pine Creek | 0.0 | 0.0 | 0.0 | 0.0 | 0.0 | 63.1 | 36.9 | 0.0 | 0.0 | 0.0 |
| 6. Canyon Creek | 12.9 | 3.2 | 0.0 | 0.0 | 0.0 | 66.1 | 17.8 | 0.0 | 0.0 | 0.0 |
| 7. Mica Creek | 0.0 | 0.0 | 0.0 | 0.0 | 0.0 | 0.0 | 100.0 | 0.0 | 0.0 | 0.0 |
| 8. Salmon River, Stibnite | 0.0 | 57.1 | 0.0 | 0.0 | 0.0 | 13.4 | 0.0 | 0.0 | 29.5 | 0.0 |
| 9. Clearwater River, Kamiah | 0.8 | 60.0 | 11.3 | 0.0 | 0.0 | 26.9 | 0.4 | 0.1 | 0.5 | 0.0 |
| 10. Little Pend Oreille River | 0.0 | 39.6 | 0.0 | 0.0 | 0.0 | 2.3 | 1.2 | 56.6 | 0.0 | 0.4 |
| 11. Union Flat Creek | 6.7 | 10.3 | 0.0 | 75.5 | 7.6 | 0.0 | 0.0 | 0.0 | 0.0 | 0.0 |
| 12. Asotin Creek | 0.1 | 0.0 | 0.0 | 36.7 | 62.6 | 0.0 | 0.6 | 0.0 | 0.0 | 0.0 |
| 13. Johnson Creek | 0.6 | 81.9 | 0.0 | 0.0 | 0.0 | 9.0 | 0.0 | 8.4 | 0.0 | 0.0 |
| 14. Saint Maries River | 3.8 | 1.4 | 7.6 | 0.0 | 0.0 | 39.9 | 47.3 | 0.0 | 0.0 | 0.0 |
| 15. Crumarine Creek | 0.0 | 100.0 | 0.0 | 0.0 | 0.0 | 0.0 | 0.0 | 0.0 | 0.0 | 0.0 |
| 16. SF Clearwater River | 0.2 | 18.7 | 0.0 | 0.0 | 0.0 | 78.2 | 2.9 | 0.0 | 0.0 | 0.0 |
| 17. Paradise Creek | 0.9 | 34.1 | 0.0 | 65.1 | 0.0 | 0.0 | 0.0 | 0.0 | 0.0 | 0.0 |
| 18. SF Palouse River | 5.8 | 28.7 | 0.1 | 58.9 | 5.8 | 0.7 | 0.0 | 0.0 | 0.0 | 0.0 |
| 19. Palouse River, Potlatch | 3.8 | 15.2 | 0.8 | 15.8 | 0.0 | 54.7 | 9.7 | 0.0 | 0.0 | 0.0 |
| 20. Tucannon River | 1.1 | 0.1 | 0.0 | 43.6 | 54.8 | 0.0 | 0.3 | 0.1 | 0.0 | 0.0 |
| 21. NF Couer D'Alene River | 3.3 | 0.0 | 0.0 | 0.0 | 0.0 | 63.7 | 33.0 | 0.0 | 0.0 | 0.0 |
| 22. Boundary Creek | 0.6 | 86.5 | 0.0 | 0.0 | 0.0 | 4.1 | 8.8 | 0.0 | 0.0 | 0.0 |
| 23. Lochsa River | 0.1 | 76.9 | 0.0 | 0.0 | 0.0 | 22.1 | 0.0 | 0.0 | 0.8 | 0.1 |
| 24. Selway River | 0.6 | 82.2 | 0.0 | 0.0 | 0.0 | 17.2 | 0.0 | 0.0 | 0.0 | 0.1 |
| 25. Salmon River, Salmon | 15.4 | 11.0 | 0.0 | 0.0 | 0.0 | 10.5 | 16.2 | 5.1 | 41.7 | 0.2 |
| 26. Palouse River, Hooper | 4.9 | 5.0 | 0.2 | 54.5 | 22.8 | 7.7 | 2.4 | 2.3 | 0.0 | 0.2 |

Since this study combines a series of flat and steep watersheds in the inland PNW with a broad spectrum of mean watershed slopes, four different fitting methods were used to evaluate the baseflow coefficients (intercept $a$ and slope $b$): (1) lower envelope (LE) with a fixed slope $b=1$; (2) organic correlation (OC); (3) ordinary least squares

 DOI 10.1007/s10040-014-1191-4

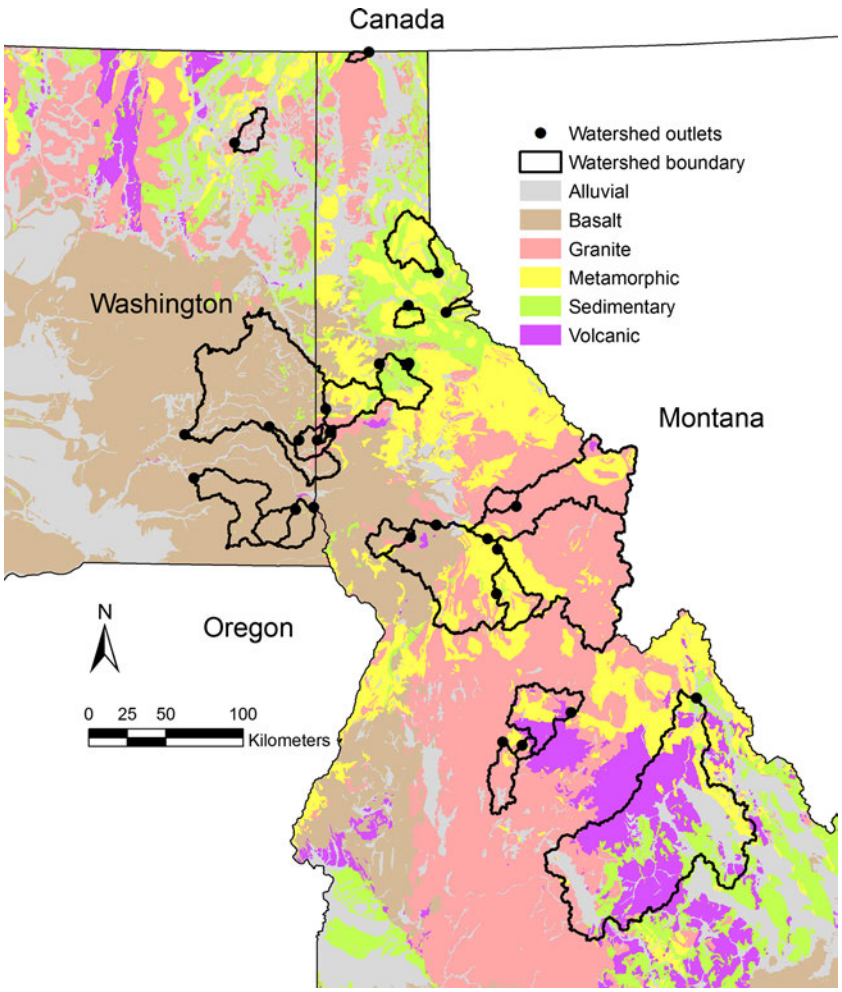


**Fig. 4** Main geology units across the study watersheds

(OLS); and (4) inverse least squares (ILS; see Appendix for more fitting method details). The lower envelope represents an advanced state of the recession process, which is characterized by small recession rates. The OC, OLS, and ILS present regressions through all the data points. The intercept $a$ can be seen as an indicator of storage volume, whereas slope $b$ is usually linked to the rate and dynamic of the recession process (Stoelzle et al. 2012). Variation in minimum annual storage $S$ [L] was conducted using Eq. (8) (Brutsaert 2008) where the $y_{L7}$ is used as a reasonable measure of minimum baseflow conditions. Minimum annual storage was computed using an average characteristic drainage timescale of 45 days ($K$) (Brutsaert 2012) and $K$ values calculated for each watershed using the aforementioned fitting models (See Table 1 in the electronic supplementary material (ESM)).

Statistically significant differences for intercepts, slopes, characteristic recession timescales, and minimum annual storage were evaluated using Tukey's multiple comparison procedure. Tukey's procedure is more conservative than the commonly used Least Significance Difference (LSD) or Student-Newman-Keuls (SNK) methods; thus, it declares fewer significant differences among $t$ population means (Ott and Longnecker 2008).

### Regression analyses

Pearson's product moment correlation coefficient, including statistical significance, was calculated between baseflow coefficients, geomorphic parameters, and climatic attributes. Regression modeling between the remaining catchment attributes and baseflow coefficients was conducted to select the best individual predictor for intercept $a$, slope $b$, and minimum annual storage $S$. A correlation matrix per individual fitting method is presented in Table 2 of the ESM.

## Results

### Estimation of baseflow recession characteristics

The overall mean intercept $a$ (lower envelope, $b$=1) for the 26 watersheds analyzed was 0.037±0.016 (1σ) $d^{-1}$ $mm^{(1-b)}$ $d^b$ with extremes ranging from 0.015 up to 0.08 $d^{-1}$ $mm^{(1-b)}$ $d^b$ (Fig. 5a). Intercepts $a$ calculated from other fitting methods (where $b$>1) are presented in Fig. 5a and Table 1 of the ESM, intercept $a$ units are represented as $mm^{(1-b)}d^b$. All distributions were positively skewed for intercepts $a$. Greater intercepts were found in steeper and forested catchments and lower values in flatter semi-arid catchments. Beck et al. (2013) presented a global analysis

 DOI 10.1007/s10040-014-1191-4

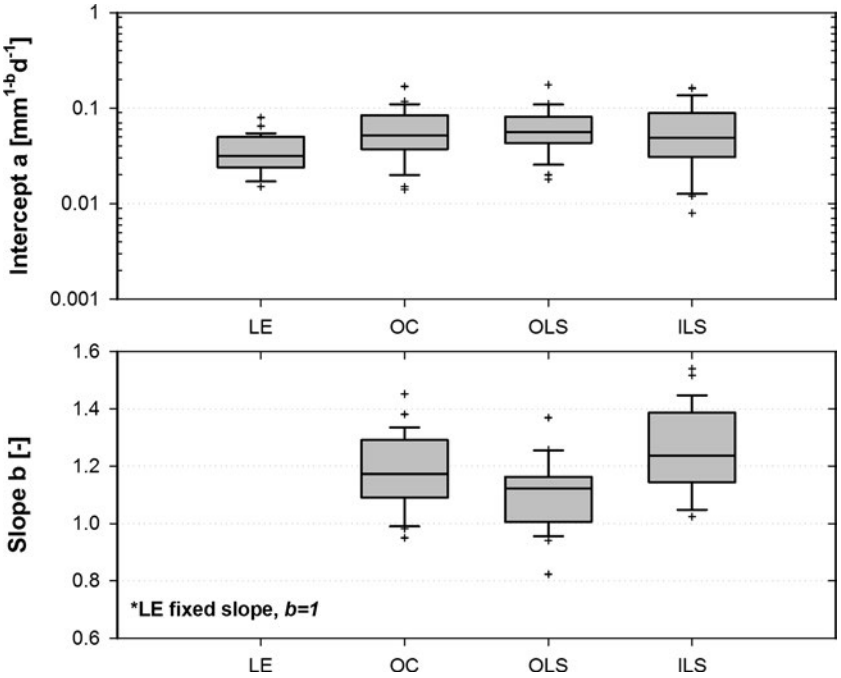


**Fig. 5** Distribution of **a** intercept *a* and **b** slope *b* for the study watersheds organized by fitting method. *Box plots* include median, 5th and 95th percentiles and error bars. *Crosses* denote the number of outliers per fitting method. *LE* lower envelope, *OC* organic correlation, *OLS* ordinary least squares, *ILS* inverse least squares

of baseflow index and recession coefficient (*a*) from streamflow observations in 3,394 catchments. The range of intercept *a* (0.02–0.08 $d^{-1}$) reported by Beck et al. (2013) for the inland PNW is consistent with the results obtained when applying the Brutsaert and Nieber (1977) lower envelope method. Slopes *b* (from OC, OLS, and ILS) varied from 0.82 up to 1.54 with a mean of 1.18±0.13 (1σ) (Fig. 5b; Table 1 ESM). Distribution of slope *b* from OLS was negatively skewed. Values of *b* from OLS and ILS were found to be significantly different ($p<0.001$).

The characteristic recession time scales *K* (i.e. LE) were fairly variable with extremes ranging from 12.5 days up to 67 days (Table S1). The mean *K* value was 33±15 days (1σ). The minimum annual storage (*S*) ranged from less than 1 mm up to 16 mm. An additional minimum annual storage condition was analyzed using a *K* value of 45 days as proposed by Brutsaert (2008) resulting in a greater median storage of 7.4 mm (Table S1).

Faster recessions and lower minimum annual storage values were found in flatter and semi-arid catchments dominated by basalt features and eolian-originated soils (e.g. Asotin Creek, Union Flat Creek, and South Fork Palouse River). Longer recessions and greater storage were found consistently where granitic, metamorphic or sedimentary rock composition is the dominant underlying geology (e.g. Crumarine Creek, Pine Creek, Mica Creek, and Saint Maries River). These catchments are also characterized by greater mean basin slopes. Individual log-log scatter plots $-dQ/dt$ versus average *Q* including all four fitting methods are shown in Fig. 6. The natural spectrum of data points observed is largely the result of non-uniform distribution of characteristics across the watersheds and the evolution of the recession process from faster depletion in channel storage (i.e. upper envelope) to lower rates of depletion from the gentler parts of the aquifer (i.e. lower envelope). Interestingly, the intercept $a_3$ calculated with a fixed slope $b=3$ (Table 1) exhibited a strong power regression with drainage area ($r^2=0.74$) (Fig. 7) and total stream length ($r^2=0.67$, not shown in Fig. 7). High variability in $a_3$ was observed for drainage areas less than 1,110 $km^2$, whereas more predictable values were found as area increased. The power exponent ($a_3=10 \times A^{-2.16}$; based on the short-time solution when $b=3$) is close to the theoretical value of −2 described by Brutsaert and Lopez (1998). This shows that $a_3$ may be used as an alternative predictor of scale-dependent hydraulic parameters such as hydraulic conductivity and drainable porosity (Table 1).

## Climatic and terrain relationships

In general, baseflow coefficients were poorly correlated with catchment scale parameters such as drainage area, perennial stream length, drainage density, and total relief (Table 2 of ESM). Intercept *a* was weakly correlated with drainage area for all fitting models (−0.26 to 0.09). The best individual regression ($r^2=0.57$) was assessed with mean basin slope as a single predictor of intercept *a* (LE) (Fig. 8a). The minimum annual storage was strongly correlated with mean basin slope (0.62–0.77). The power regression ($r^2=0.75$) between minimum annual storage (*S*) versus mean basin slope is shown in Fig. 8b.

The characteristic recession timescale (*K*) shows a similar pattern found with intercept *a* where the best correlation is linked to the mean basin slope; however, due

 DOI 10.1007/s10040-014-1191-4

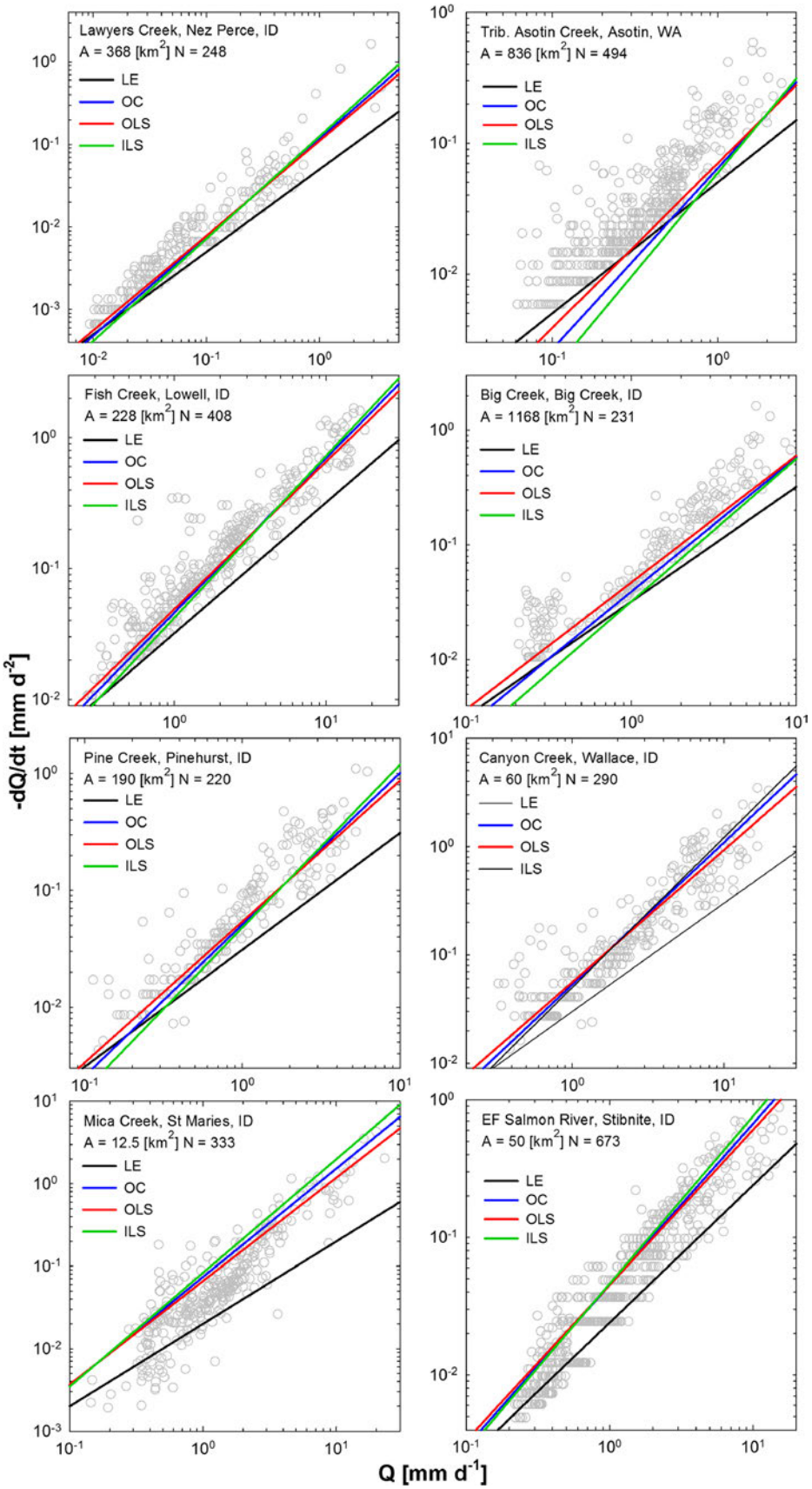


**Fig. 6** Recession plots (log-log scale) showing $-dQ/dt$ [mm $d^{-2}$] versus the average $Q$ [mm $d^{-1}$] and four different fitting procedures. *Black line* represents the lower envelope (*LE*) ($b=1$) method. Organic correlation (*OC*) is represented by *blue lines*. Ordinary (*OLS*) and inverse least squares (*ILS*) are represented by *red* and *green lines*, respectively. Plots are organized by the increasing number of record years (See Table 2)

 DOI 10.1007/s10040-014-1191-4

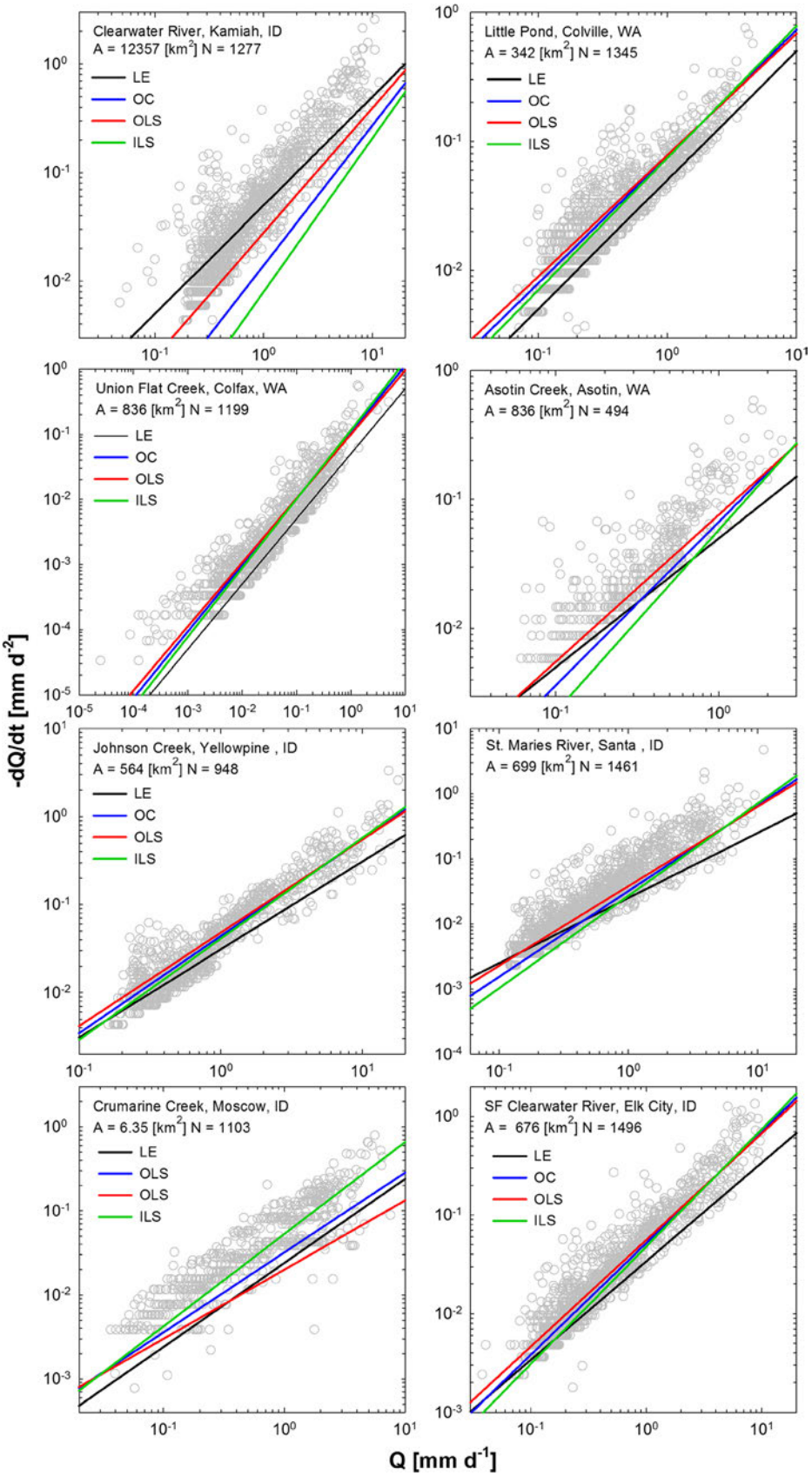


**Fig. 6** continued.

 DOI 10.1007/s10040-014-1191-4

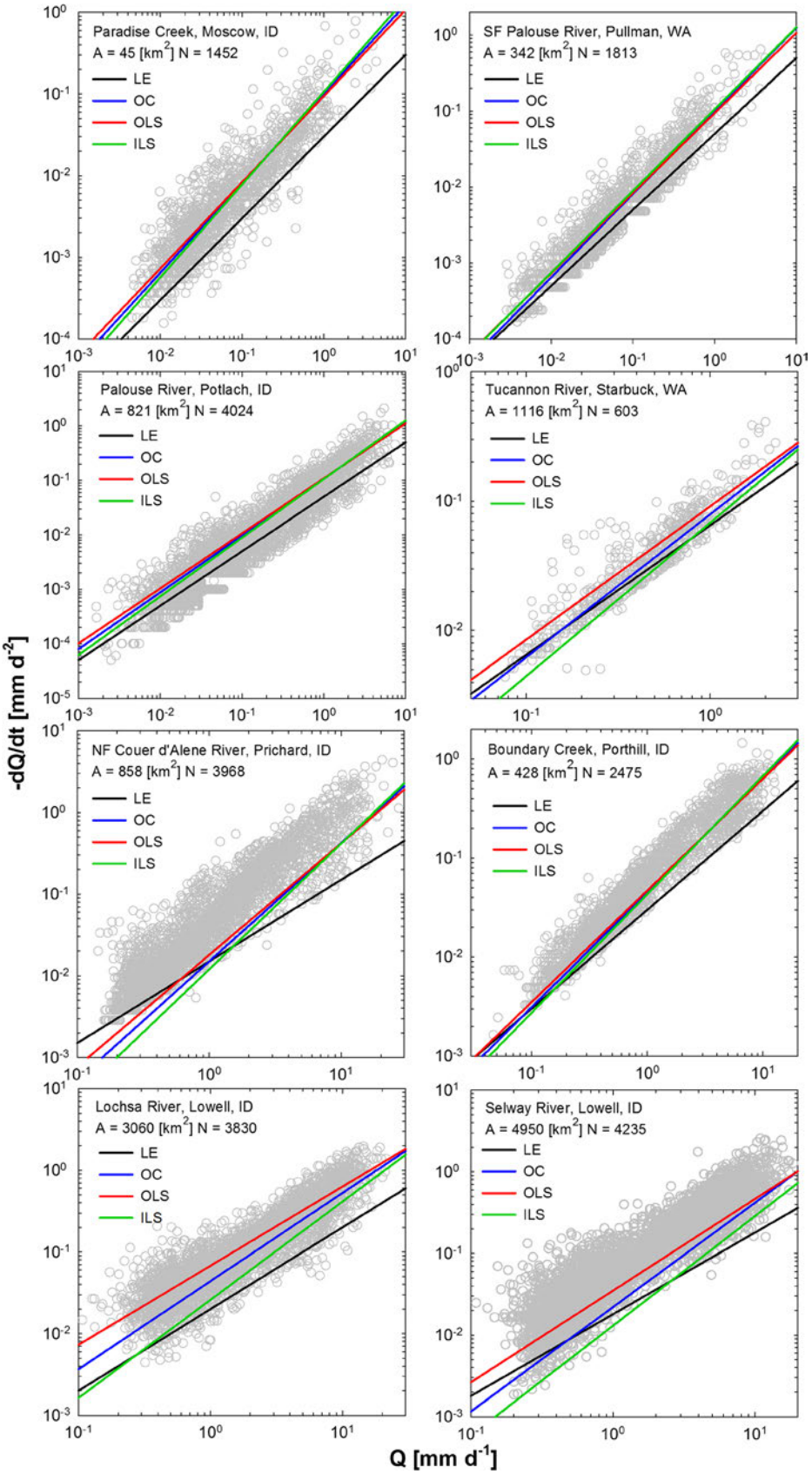


**Fig. 6** continued.

 DOI 10.1007/s10040-014-1191-4

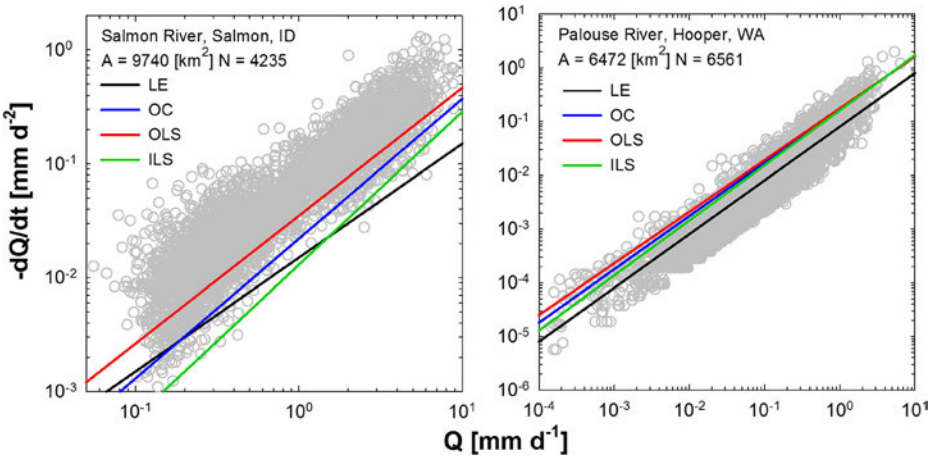


**Fig. 6** continued.

to their high collinearity, $K$ was not used in the regression analysis. Brutsaert's approach using a constant $K$ of 45 days to calculate storage for watersheds with area greater than 100 km$^2$ tends to overestimate the minimum annual storage in comparison with the fitting methods.

The aridity index (AI=mean annual $P$/mean potential ET) ranged from 1.09 up to 2.70. A moderate power regression ($a_{mean}$=0.051AI$^{-0.89}$; $r^2$=0.40) was found between mean intercept $a$ and the aridity index (Fig. 9) Semi-arid watersheds with greater ET exhibited lower aridity index values; therefore, lower recession timescales. Forested areas with greater mean annual precipitation and lower ET tend to have longer recession depletions and greater minimum annual storage. This is similar to a relationship reported by Peña-Arancibia et al. (2010) in a study of 167 subtropical and tropical watersheds.

## Discussion

As baseflow will likely continue to decrease in the coming century in the inland PNW, understanding the processes that impact baseflow at catchment scales and over a range of climate gradients and geology units can inform management of the ecosystem services that society and nature derive from watersheds. This study analyzed a wide range of storage–discharge relationships to attempt a regionalized baseflow characterization in the inland Pacific Northwest that can be translated to ungauged basins sharing similar climate and underlying geological features.

No significant relationship was found between drainage area and baseflow coefficients $a$ and $b$ (i.e. obtained from the linear lower envelop method). Similar findings have been reported elsewhere (Lacey and Grayson 1998; Peña-Arancibia et al. 2010; Stoelzle et al. 2012). Generally, small intercepts were associated with longer characteristic recession times and larger minimum annual storage. Catchments with underlying basalt tended to be drier, had flatter slopes,

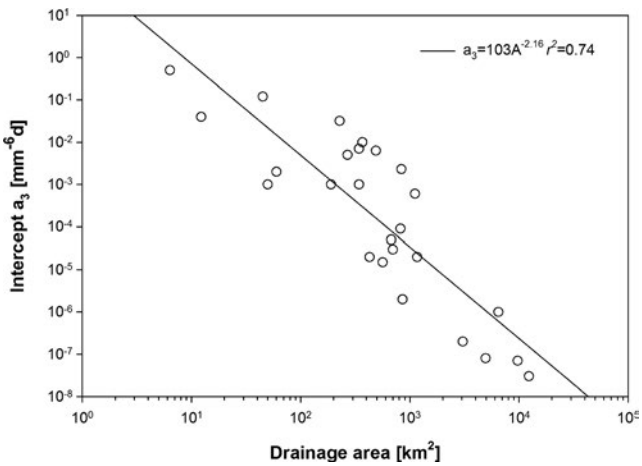


**Fig. 7** Intercept $a_3$ versus drainage area $A$ (log-log scale). *Solid line* is the best-fit power curve for the observed data

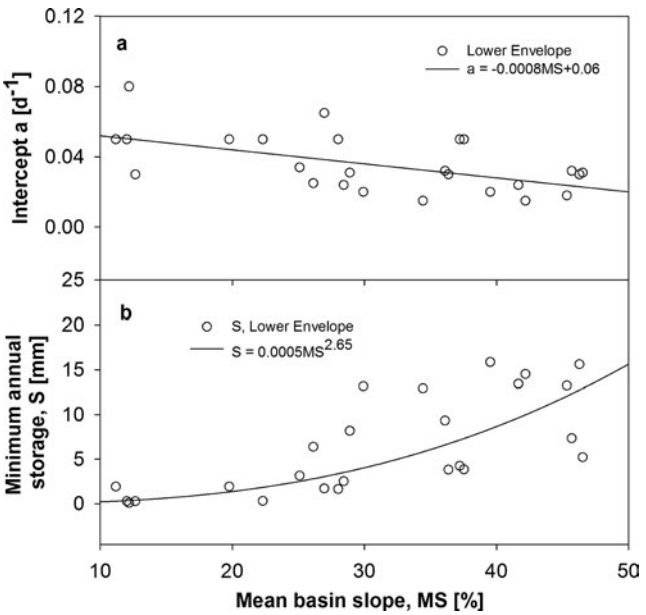


**Fig. 8** Scatter plots of mean basin slope versus **a** intercept $a$ and **b** minimum annual storage $S$. *Open circles* denote values for intercept $a$ and for $S$ obtained with the lower envelope method


DOI 10.1007/s10040-014-1191-4

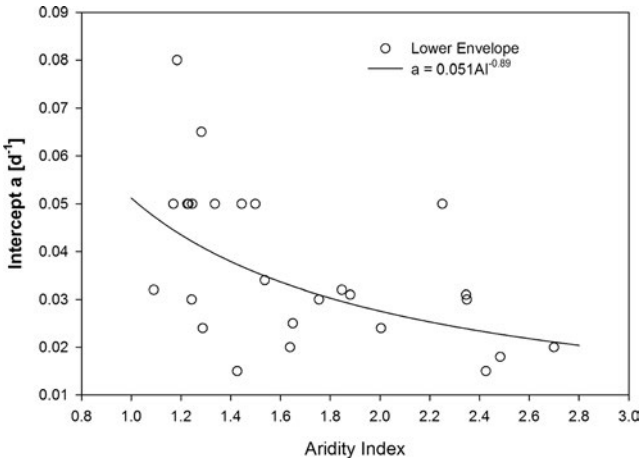


**Fig. 9** Scatter plot of aridity index versus intercept *a* (*–LE* lower envelope)

and exhibited shorter recession times and lower storages values. These watersheds are also characterized by a lower aridity index (i.e. lower *P* and greater ET) that may accelerate the rate of recession. The potential for increased ET with warming climates could lead to even higher recession depletions in these areas affecting irrigation activities and the thermal regime of aquatic habitats. Forested areas resulted in longer recession times and greater minimum storage. These near-natural forested areas, mainly underlain by granitic, metamorphic, and sedimentary features, with lower hydraulic conductivity relative to fractured basalt, may play a significant role in the groundwater storage and baseflow contributions (Fig. 10). It has been reported that the power law coefficient *a* depends on the initial storage in the basin (Biswal and Marani 2014; Biswal and Kumar 2014a, b), therefore, if a basin is more wet, '*a*' will be smaller, and vice versa. Additionally, the mean basin slope appeared to be the best estimator of intercept *a* in a power function following by the climatic aridity index. This could potentially be used to characterize baseflow conditions in ungauged basins across the inland Pacific Northwest.

Several authors have identified that the variability of slope *b* could bring useful information about aquifer behavior. In this study, watersheds located in eastern Washington and western Idaho dominated by flatter landscapes, shallow eolian-originated soils, and basalt geology exhibited a predominant linear behavior. In contrast, watersheds in northern and east-central Idaho dominated by steeper forested terrains resulted in greater slopes that may be a result of more active channel storage and lateral flow pathways. Overall, slope *b* was in the range of literature values (Brutsaert and Lopez 1998; Palmroth et al. 2010; Biswal and Marani 2010; Wang 2011; Shaw and Riha 2012). Since the values of *b* evolve and denote distinct stages of the recession phenomena, when analyzed as individual recession events (Shaw and Riha 2012), an analysis of all recession events might mask other relationships with geomorphic characteristics of the riparian aquifers that do not emerge at the watershed scale.

Probably, the most useful application of knowing the characteristic recession timescale of any catchment is the estimation of storage conditions. It is well known that long-term records of groundwater storage are scarce within the inland Pacific Northwest and in many regions of the world; therefore, estimation of minimum annual storage becomes critical for noteworthy diagnoses of water availability under different land use and climate change scenarios. This analysis suggested that watersheds located in eastern Washington and northwestern Idaho due to a combination of several factors such as flatter basalt landscapes, low precipitation and high ET rate could confront even shorter recession times and less

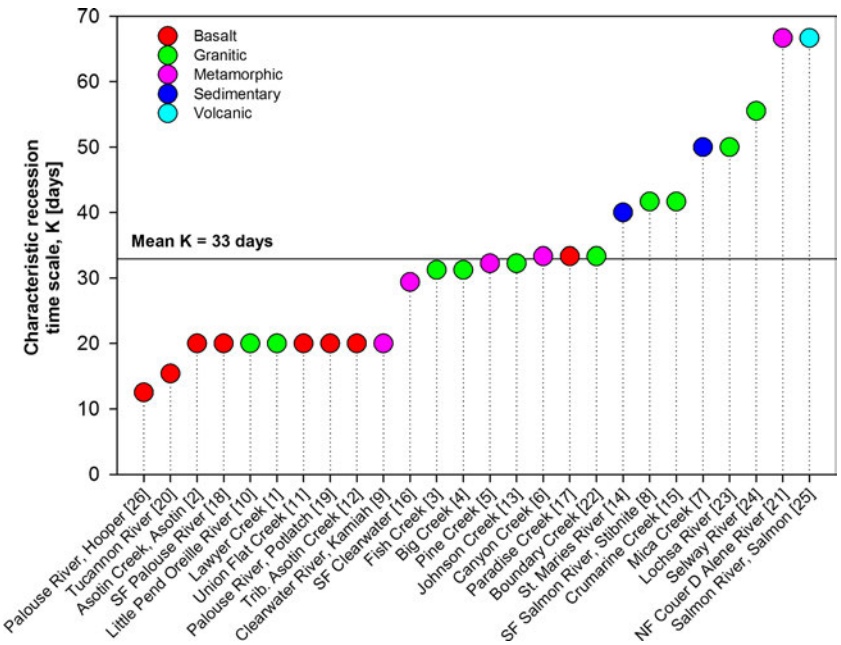


**Fig. 10** Relationship of characteristic recession time scale *K* [days] and main underlying geology among the study watersheds

 DOI 10.1007/s10040-014-1191-4

than 1 mm of minimum annual storage in several water catchments. Lower storage can result in decreased summer flows that with the same pollutant inputs could lead to declining water quality, recreation opportunities, and availability of ecological habitat for endangered species such as salmonids. Additionally, forested areas of northern and eastern Idaho characteristically have longer recession times and greater minimum annual storage volumes with $S$ values greater than 20 mm.

## Conclusions

Baseflow recession characteristics and their relationship to landscape, geomorphic, and climatic attributes have been a matter of debate among the hydrology community for several decades. Despite this debate, the spatial heterogeneity and intrinsic complexity of baseflow processes have turned the attention of researchers to (1) physically based efforts that permit the parameterization of hydraulic parameters over meso ($10^2$ km$^2$) and large ($10^3$ km$^2$) catchment areas and (2) regional analyses that provide a systematic perspective of water sustainability (i.e. surface and groundwater resources) for the upcoming decades. For the inland Pacific Northwest, water managers, understanding how the combination of potentially greater ET, earlier spring runoff, and prolonged droughts will affect baseflow regimes has become an imperative.

The long-term trend of declining summer baseflow in the PNW and the threat of continued and potentially more significant declines in the future due to climate change depicts future hydro-climate scenarios that may translate in severe consequences to the demand for groundwater for food production, electricity generation, clean drinking water, and recreation. This increase in demand may lead to individual and inter-state water rights debates, and disruption of ecological attributes (e.g. high water temperatures, low dissolved oxygen concentrations) during summer flows that are critical to many ecosystems such as steelhead/salmon rearing habitats.

The findings of this study indicate that baseflow coefficients are not strongly related with drainage scale. The most significant parameter controlling the natural release of water as baseflow was the mean basin slope. The climatic aridity index also could be a useful estimator of baseflow parameters. The findings suggest that watersheds located in eastern Washington and northwestern Idaho due to a combination of several factors such as flatter basalt landscapes, low precipitation, and high ET rates could experience even faster recession times and less than 1 mm of minimum annual storage.

The baseflow recession characteristics provided in this study may enhance physically based modeling by reducing the use of trial and error approaches to calibrate baseflow or deep percolation conditions. By knowing baseflow characteristics such as minimum annual storage and recession timescales, land managers and environmental agencies could prioritize efforts and resources in areas where potential future droughts may drastically affect overall ecosystems services.

**Acknowledgements** This project was funded by the joint venture agreement (No. 10-JV-11221634-252) between USDA-Forest Service Rocky Mountain Research Station and the University of Idaho. The authors thank the insights and useful comments from two anonymous reviewers.

## Appendix 1

To estimate the baseflow coefficients (i.e. $a$ and $b$), four different fitting methods were used: lower envelope, the organic correlation technique (Eqs. 9 and 10), ordinary (Eqs. 11 and 12) and inverse (Eqs. 13 and 14) least square estimation. There is some argument over the best technique for fitting a line through data: either ordinary least squares (the commonly used approach in statistics), inverse least squares, or the organic correlation technique described by Hirsch and Gilroy (1984). The ordinary least squares technique determines a line which minimizes the sum of the square errors in the vertical or y direction. This is the preferred method for estimating a particular value of $y$, given a value of $x$ where $x$ is measured without error (Hirsch and Gilroy 1984). Conversely, the inverse least squares method is used to estimate $x$ (assumed measured without error) given a value of $y$. The organic correlation technique minimizes the sum of the squared geometric means of the distances in both the vertical and horizontal directions. This technique is not suited for minimizing estimation errors, but is most applicable for establishing equivalence between $x$ and $y$. In addition, Brutsaert (2005) emphasized that in hilly watersheds, it may be advisable to analyze an average value of the baseflow coefficients.

$$\alpha = \left[\text{average}\left(\frac{dQ}{dt}\right) - \text{average}(Q)\right] x\ \text{sign}\left[\text{correl}\left(Q, \frac{dQ}{dt}\right)\right] \times \frac{\text{StdevP}\left(\frac{dQ}{dt}\right)}{\text{StdevP}(Q)} \tag{9}$$

$$b = \text{sign}\left[\text{correl}\left(Q, \frac{dQ}{dt}\right)\right] \times \frac{\text{StdevP}\left(\frac{dQ}{dt}\right)}{\text{StdevP}(Q)} \tag{10}$$

$$\alpha = \left[\text{average}\left(\frac{dQ}{dt}\right) - \text{average}(Q)\right] \times \text{correl}\left(Q, \frac{dQ}{dt}\right) \times \frac{\text{StdevP}\left(\frac{dQ}{dt}\right)}{\text{StdevP}(Q)} \tag{11}$$

 DOI 10.1007/s10040-014-1191-4

$$b = \text{correl}\left(Q, \frac{dQ}{dt}\right) \times \frac{\text{StdevP}\left(\frac{dQ}{dt}\right)}{\text{StdevP}(Q)} \quad (12)$$

$$\alpha = \left[\text{average}\left(\frac{dQ}{dt}\right) - \text{average}(Q)\right] / \text{correl}\left(Q, \frac{dQ}{dt}\right) \times \frac{\text{StdevP}\left(\frac{dQ}{dt}\right)}{\text{StdevP}(Q)} \quad (13)$$

$$b = \text{StdevP}\left(\frac{dQ}{dt}\right) / \text{correl}\left(Q, \frac{dQ}{dt}\right) / \text{StdevP}(Q) \quad (14)$$

where StdevP is the standard deviation of the population.

## References


Ajami H, Troch P, Maddock T, Meixner T, Eastoe C (2011) Quantifying mountain block recharge by means of catchment-scale storage-discharge relationships. Water Resour Res 47:W04504. doi:10.1029/2010WR009598

Arnell NW, Gosling SN (2013) The impacts of climate change on river flow regimes at the global scale. J Hydrol 486:351–364. doi:10.1016/j.jhydrol.2013.02.010

Bates B C, Kundzewicz Z W, Wu S, Palutikof J P (2008) Climate change and water. Technical Paper of the Intergovernmental Panel on Climate Change, IPCC Secretariat, Geneva, 210 pp

Beck HE, van Dijk AIJM, Miralles DG, de Jeu RAM, Bruijnzeel LA, McVicar TR, Schellekens J (2013) Global patterns in base flow index and recession based on streamflow observations from 3,394 catchments. Water Resour Res 49:7843–7863. doi:10.1002/2013WR013918

Berghuijs WR, Woods RA, Hrachowitz M (2014) A precipitation shift from snow towards rain leads to a decrease in streamflow. Nat Clim Chang 4:583–586. doi:10.1038/NCLIMATE2246

Biswal B, Marani M (2010) Geomorphological origin of recession curves. Geophys Res Lett 37:L24403. doi:10.1029/2010GL045415

Biswal B, Marani M (2014) 'Universal' recession curves and their geomorphological interpretation. Adv Water Resour 65:34–42. doi:10.1016/j.advwatres.2014.01.004

Biswal B, Nagesh Kumar D (2014a) Study of dynamic behavior of recession curves. Hydrol Process 28:784–792. doi:10.1002/hyp.9604

Biswal B, Nagesh Kumar D (2014b) What mainly controls recession flows in river basins? Adv Water Resour 65:25–33. doi:10.1016/j.advwatres.2014.01.001

Bloomfield JP, Allen DJ, Griffiths KJ (2009) Examining geological controls on baseflow index (BFI) using regression analysis: an illustration from the Thames Basin, UK. J Hydrol 373:164–176. doi:10.1016/j.jhydrol.2009.04.025

Boussinesq J (1877) Essai sur la theorie des eaux courantes: du movement non permanent des eaux souterraines [Essay on the theory of running waters: from non-permanent movement of groundwater]. Acad Sci Inst Fr 23:252–260

Boussinesq J (1903) Sur le débit, en temps de sécheresse, d' une source alimentée par une nappe d'eaux infiltration [On the flow in times of drought, spring fed by groundwater outflow]. C R Seanes Acad 136:1511–1517

Boussinesq (1904) Recherches theories sur l'écoulement des nappes d'eau infiltrées dans le sol et sur débit sources [Research theories on groundwater flow and flowpaths]. J Math Pures Appl 10:5–78

Brandes D, Hoffman J, Mangarillo JT (2005) Baseflow recession rates, low flows, and hydrologic features of small watersheds in Pennsylvania, USA. Am Water Res Assoc 41(5):1177–1186. doi:10.1111/j.1752-1688.2005.tb03792.x

Brutsaert W (2005) Hydrology: an introduction. Cambridge University Press, Cambridge, UK, 605 pp

Brutsaert W (2008) Long-term groundwater storage trends estimated from streamflow records: climatic perspective. Water Resour Res 44:W022409. doi:10.1029/2007WR006518

Brutsaert W (2010) Annual drought flow and groundwater storage trends in the eastern half of the United States during the past two-third century. Theor Appl Climatol 100:93–103. doi:10.1007/s00704-009-0180-3

Brutsaert W (2012) Are the North American deserts expanding? Some climate signals from groundwater storage conditions. Ecohydrology 5:541–549. doi:10.1002/eco.263

Brutsaert W, Lopez JP (1998) Basin-scale geohydrologic drought flow features of riparian aquifers in the southern Great Plains. Water Resour Res 34(2):233–240. doi:10.1029/97WR03068

Brutsaert W, Nieber J (1977) Regionalized drought flow hydrographs from a mature glaciated plateau. Water Resour Res 13(3):637–643. doi:10.1029/WR013i003p00637

Brutsaert W, Sugita M (2008) Is Mongolia's groundwater increasing or decreasing? The case of the Kherlen River basin. Hydrol Sci 53:1221–1229. doi:10.1623/hysj.53.6.1221

Clark GM (2010) Changes in patterns of streamflow from unregulated watersheds in Idaho, western Wyoming, and northern Nevada. Am Water Res Assoc 46(3):486–497. doi:10.1111/j.1752-1688.2009.00416.x

Dams J, Salvadore E, van Daele T, Ntegeka V, Willems P, Batelaan O (2012) Spatio-temporal impact of climate change on the groundwater system. Hydrol Earth Syst Sci 16:1517–1531. doi:10.5194/hessd-8-10195-2011

Del Genio AD, Lacis AA, Ruedy RA (1991) Simulations of the effect of a warmer climate on atmospheric humidity. Nature 351:382–385. doi:10.1038/351382a0

Döll P, Zhang J (2010) Impact of climate change on freshwater ecosystems: a global-scale analysis of ecologically relevant river flow alterations. Hydrol Earth Syst Sci 14(5):783–799. doi:10.5194/hessd-7-1305-2010

Döll P, Müller-Schmied H (2012) How is the impact of climate change on river flow regimes related to the impact on mean annual runoff? A global-scale analysis. Environ Res Lett 7(1). doi:10.1088/1748-9326/7/1/014037

Durack P, Wijffels SE, Matear RJ (2012) Ocean salinities reveal strong global water cycle intensification during 1950 to 2000. Science 336:455–458. doi:10.1126/science.1212222

Elsner MM, Cuo L, Voisin N, Deems JS, Hamlet AF, Vano JA, Mickelson K, Lee S, Lettenmaier DP (2010) Implications of 21st century climate change for the hydrology of Washington State. Clim Chang 102:225–260. doi:10.1007/s10584-010-9855-0

Fu G, Barber ME, Chen S (2010) Hydro-climatic variability and trends in Washington State for the last 50 years. Hydrol Process 24(7):866–878. doi:10.1002/hyp.7527

Hall FR (1968) Base-flow recession: a review. Water Resour Res 4(5):973–983. doi:10.1029/WR004i005p00973

Hirsch RM, Gilroy EJ (1984) Methods of fitting a straight line to data: examples in water resources. Water Resour Bull 20:705–711. doi:10.1111/j.1752-1688.1984.tb04753.x

Huntington TG (2006) Evidence for intensification of the global water cycle: review and synthesis. J Hydrol 319:83–95. doi:10.1016/j.jhydrol.2005.07.003

Kirchner JW (2009) Catchments as simple dynamical systems: catchment characterization, rainfall-runoff modeling, and doing hydrology backward. Water Resour Res 45:W02429, 34 pp. doi:10.1029/2008WR006912

Lacey GC, Grayson RB (1998) Relating baseflow to catchment properties in south-eastern Australia. J Hydrol 204:231–250. doi:10.1016/S0022-1694(97)00124-8

Leppi JC, DeLuca TH, Harrar SW, Running SW (2012) Impacts of climate change on August stream discharge in the Central-Rocky Mountains. Clim Chang 112:997–1014. doi:10.1007/s10584-011-0235-1

Luce CH, Holden ZA (2009) Declining annual streamflow distributions in the Pacific Northwest United States, 1948–2006. Geophys Res Lett 36:L16401. doi:10.1029/2009GL039407

Mayer TD (2012) Controls of summer stream temperature in the Pacific Northwest. J Hydrol 475:323–335. doi:10.1016/j.jhydrol.2012.10.012

McCabe GJ, Clark MP (2005) Trends and variability in snowmelt runoff in the western United States. J Hydrometeorol 6(4):476–482. doi:10.1175/JHM428.1

Mendoza GF, Steenhuis TS, Walter MT, Parlange JY (2003) Estimating basin-wide hydraulic parameters of a semi-arid mountainous watershed by recession-flow analysis. J Hydrol 279:57–69. doi:10.1016/S0022-1694(03)00174-4

Miles EL, Snover AK, Hamlet AF, Callahan B, Fluharty D (2000) Pacific Northwest regional assessment: the impacts of climate variability and climate change on the water resources of the Columbia River basin. Am Water Res Assoc 36(2):399–420

Milly PCD, Dunne KA, Vecchia AV (2005) Global pattern of trends in streamflow and water availability in a changing climate. Nat Lett 438:347–350

Mote PW (2003) Trends in snow water equivalent in the Pacific Northwest and their climatic causes. Geophys Res Lett 30:1601. doi:10.1029/2003GL017258

Mote PW, Salathé EP (2010) Future climate in the Pacific Northwest. Clim Chang 102(1–2):29–50. doi:10.1007/s10584-010-9848-z

National Oceanic and Atmospheric Administration (2011) National Climate Data Center. Available at: http://www.ncdc.noaa.gov/. Accessed February 20, 2011

Nijssen B, O'Donnell GM, Hamlet AF, Lettenmaier DP (2001) Hydrologic sensitivity of global rivers to climate change. Clim Chang 50:143–175. doi:10.1023/A:1010616428763

Ott R, Longnecker M (2008) An introduction to statistical methods and data analysis. Cenage Learning, Boston, MA, 1280 pp

Pale EJ (2002) Flood risk and flood management. J Hydrol 267:2–11. doi:10.1016/S0022-1694(02)00135-X

Palmroth S, Katul GG, Hui D, McCarthy HR, Jackson RB, Oren R (2010) Estimation of long-term basin scale evapotranspiration from streamflow time series. Water Resour Res 46:W10512. doi:10.1029/2009WR008838

Parlange J, Stagnitti F, Heilig A, Szilagyi J, Parlange M, Steenhuis T, Hogarth W, Barry D, Li L (2001) Sudden drawdown and drainage of a horizontal aquifer. Water Resour Res 37:2097–2101

Peña-Arancibia JL, van Dijk AIJM, Mulligen M, Bruijzeel LA (2010) The role of climatic and terrain attributes in estimating baseflow recession in tropical catchments. Hydrol Earth Syst Sci 7:4059–4087. doi:10.5194/hessd-7-4059-2010

Polubarinova-Kochina PY (1962) Theory of groundwater movement. Princeton University Press, Princeton, NJ. doi:10.1029/2000WR000189

Poole GC, Berman CH (2001) An ecological perspective on in-stream temperature: natural heat dynamics and mechanisms of human-caused thermal degradation. Environ Manag 27(6):787–802. doi:10.1007/s002670010188

Price K (2011) Effects of watershed topography, soils, land use, and climate on baseflow hydrology in humid regions: a review. Prog Phys Geogr 35(4):465–492. doi:10.1177/0309133311402714

Rupp DE, Selker JS (2006) Information, artifacts, and noise in *dQ/dt-Q* recession analysis. Adv Water Resour 29:154–160. doi:10.1016/j.advwatres.2005.03.019

Sánchez-Murillo R, Brooks ES, Sampson L, Boll J, Wilhelm F (2013) Ecohydrological analysis of steelhead (*Oncorhynchus mykiss*) habitat in an effluent dependent stream in the Pacific Northwest, USA. Ecohydrology. doi:10.1002/eco.1376

Shaw SB, Riha SJ (2012) Examining individual recession events instead of a data cloud: using a modified interpretation of dQ/dt–Q streamflow recession in glaciated watersheds to better inform models of low flow. J Hydrol 434–435:46–54. doi:10.1016/j.jhydrol.2012.02.034

Smakhtin VU (2001) Low flow hydrology: a review. J Hydrol 240:147–186. doi:10.1016/S0022-1694(00)00340-1

Stewart IT, Cayan DR, Dettinger MD (2005) Changes toward earlier streamflow timing across Western North America. Climate 18:1136–1155. doi:10.1175/JCLI3321.1

Stoelzle M, Stahl K, Weiler M (2012) Are streamflow recession characteristics really characteristic? Hydrol Earth Syst Sci 9:10563–10593. doi:10.5194/hessd-9-10563-2012

Szilagyi J, Parlange MB, Albertson JD (1998) Recession flow analysis for aquifer parameter determination. Water Resour Res 34(7):1851–1857. doi:10.1029/98WR01009

Tallaksen LM (1995) A review of baseflow recession analysis. J Hydrol 165:349–370. doi:10.1016/0022-1694(94)02540-R

Tang QH, Lettenmaier DP (2012) 21st century runoff sensitivities of major global river basins. Geophys Res Lett 39:L06403. doi:10.1029/2011gl050834

Troch P, De Troch F, Brutsaert W (1993) Effective water table depth to describe initial conditions prior to storm rainfall in humid regions. Water Resour Res 29(02):427–434. doi:10.1029/92WR02087

UNESCO (2005) International flood initiative. Available at: http://www.ifi-home.info/. Accessed February 20, 2011

United States Geological Survey (2011) National Water Information System. Available at: http://waterdata.usgs.gov/usa/nwis/rt. Accessed February 20, 2011

van Dijk AIJM (2010) Climate and terrain factors explaining streamflow response and recession in Australian catchments. Hydrol Earth Syst Sci 14:159–169. doi:10.5194/hess-14-159-2010

van Kirk RW, Naman SW (2008) Relative effects of climate and water use on base-flow trends in the Lower Klamath basin. Am Water Res Assoc 44(4):1032–1052. doi:10.1111/j.1752-1688.2008.00212.x

Vogel RM, Kroll CN (1992) Regional geohydrologic-geomorphic relationships for the estimation of low-flow statistics. Water Resour Res 28(9):2451–2458. doi:10.1029/92WR01007

Wang D (2011) On the base flow recession at the Panola Mountain Research Watershed, Georgia, USA. Water Resour Res 47:W03527. doi:10.1029/2010WR009910

Wang D, Cai X (2009) Detecting human interferences to low flows through base flow recession analysis. Water Resour Res 45:W07426. doi:10.1029/2009WR007819

Wang D, Cai X (2010a) Comparative study of climate and human impacts on seasonal baseflow in urban and agricultural watersheds. Geophys Res Lett 37:L06406. doi:10.1029/2009GL041879

Wang D, Cai X (2010b) Recession slope curve analysis under human interferences. Adv Water Resour 33(2010):1053–1061. doi:10.1016/j.advwatres.2010.06.010

Wittenberg H (1999) Baseflow recession and recharge as nonlinear storage processes. Hydrol Process 13:715–726. doi:10.1002/(SICI)1099-1085(19990415)13:5<715::AID-HYP775>3.0.CO;2-N

Wittenberg H (2003) Effects of season and man-made changes on baseflow and flow recession: case studies. Hydrol Process 17:2113–2123. doi:10.1002/hyp.1324

Wolock D (2003) Base-flow index grid for the conterminous United States. US Geol Surv Open-File Rep 03-146. Digital dataset available on http://water.usgs.gov/GIS/dsdl/bfi48grd.zip. March 2011

Zecharias Y, Brutsaert W (1988) Recession characteristics of groundwater outflow and base flow from mountainous watersheds. Water Resour Res 24(10):1651–1658. doi:10.1029/WR024i010p01651

Zhou YP, Kuan-Man X, Sud YC, Betts AK (2011) Recent trends of the tropical hydrological cycle inferred from Global Precipitation Climatology Project and International Satellite Cloud Climatology Project data. Geophys Res 116:D09101. doi:10.1029/2010JD015197